# scientific reports



# OPEN

# Bauhinia coccinea extract prevents memory loss induced by scopolamine through activation of antiapoptotic and antioxidant pathways in mice

Eunjin Sohn¹, Bu-Yeo Kim¹, Yu Jin Kim¹, Joo-Hwan Kim² & Soo-Jin Jeong¹□

Alzheimer's disease (AD) is characterized by oxidative stress-mediated memory dysfunction and neuronal cell death. This study investigated the effects of an ethanol extract from Bauhinia coccinea (EEBC) on memory impairment and neuronal damage in a memory deficit mouse model. EEBC was administered to ICR mice at doses of 50, 100, or 200 mg/kg daily for 3 weeks. Cognitive impairment was induced via scopolamine (SCO) injection. Brain tissues were analyzed for acetylcholine (ACh) levels, acetylcholinesterase (AChE) activity, neuronal apoptosis, and antioxidant markers. Behavioral tests showed that SCO injection induced memory loss, whereas EEBC significantly ameliorated SCO-mediated memory impairment. EEBC regulated the cholinergic system by decreasing ACh levels and enhancing AChE activity. NissI staining and immunohistochemistry for NeuN showed that EEBC exerted neuroprotective effects in SCO-injected mice brains. Moreover, EEBC significantly reduced the number of terminal deoxynucleotidyl transferase dUTP nick end labeling-positive apoptotic cells increased by SCO treatment. EEBC also reversed the SCO-induced changes in apoptosis-related protein expression in brain tissues. Furthermore, EEBC significantly reduced malondialdehyde levels and activated catalase in SCO-administered brains. Quantitative RNA sequencing showed involvement of lipid metabolism in EEBC memory function regulation. Thus, EEBC is a promising candidate for attenuating AD progression as it targets the cholinergic system and neuronal apoptosis.

**Keywords** Alzheimer's disease, *Bauhinia coccinea*, Memory dysfunction, Neuronal apoptosis, Antioxidant activity

Memory impairment is a critical symptom that poses significant challenges to individuals and society, associated with aging and neurodegenerative diseases including Alzheimer's disease (AD), Parkinson's disease, and amyotrophic lateral sclerosis<sup>1</sup>. The population with or at risk of AD is rapidly increasing worldwide, underscoring the urgent need to develop effective treatments. The cholinergic system plays a key role in the pathogenesis of AD. Acetylcholinesterase (AChE) metabolizes the neurotransmitter acetylcholine (ACh) at the synaptic cleft, resulting in memory and cognitive impairment<sup>2-4</sup>. The U.S. Food and Drug Administration (FDA) has approved several therapeutic drugs for AD that target AChE, including donepezil, tacrine, rivastigmine, and galantamine. These drugs help alleviate symptoms and delay the progression of mild cognitive impairment or mild-to-severe AD. However, they do not provide a cure<sup>5</sup>, underscoring the need for safer and more effective alternatives. Despite these limitations, the cholinergic system remains a viable target for the development of AD treatments.

Accumulating data have highlighted the potential of various natural products, including medicinal plant extracts, in neuroprotection and memory enhancement in AD-like experimental models. For instance, Carranzoni et al. recently reported that *Manihot esculenta* Crantz (Cassava) leaf extract prevents impairment and antioxidant dysfunction in amyloid beta  $(A\beta)$ -injected mice<sup>6</sup>. Ibrahim et al. demonstrated that *Erigeron bonariensis* extract has neuroprotective potential in ovariectomized rats with D-galactose-induced memory deficit<sup>7</sup>. Our group also demonstrated the potential of extracts from *Annona atemoya*, *Ficus erecta* Thunb, and

<sup>1</sup>Korean Medicine Convergence Research Division, Korea Institute of Oriental Medicine, Daejeon 34054, South Korea. <sup>2</sup>Department of Life Science, Gachon University, Seongnam, Gyeonggi-do 13120, South Korea. <sup>⊠</sup>email: sjijeong@kiom.re.kr

*Elaeagnus glabra* f. *oxyphylla* as therapeutics for AD and related diseases<sup>8–10</sup>. More importantly, natural products offer promising advantages because of their safety profiles and multifaceted biological activities<sup>11,12</sup>.

Our recent findings demonstrated the ability of *Bauhinia coccinea* extract to inhibit AD biomarkers in vitro<sup>13</sup>. *B. coccinea* is a flowering plant in the family Fabaceae that thrives in tropical regions of Southeast Asia, including Thailand and India. The pharmacological effects of *B. coccinea* have rarely been reported compared to other *Bauhinia* genera<sup>14-16</sup>. *B. purpirea* Linn. extract exerts anti-arthritic activity and cerebroprotective actions in animal models<sup>2,17</sup>. *B. variegate* Linn. was reported to have radical scavenging potential and neuroprotective effects<sup>18,19</sup>. *B. championii* Benth. extract attenuated the inflammatory reaction and nuclear factor kappa B (NF-κB) in an arthritis model and mediated cell cycle arrest in colorectal cancer cells<sup>20-22</sup>. Additionally, *B. forficata* Link exhibits anti-diabetic, anti-microbial, antioxidant, genoprotective, and hypoglycemic activity<sup>23-26</sup>.

The present study aimed to investigate the effect of *B. coccinea* on memory impairment to validate our previous findings and to identify the underlying molecular mechanisms of its anti-AD properties using a scopolamine (SCO)-induced memory deficit mouse model. The hypothesis was that *B. coccinea* mitigates memory impairment, neuronal damage, and oxidative stress induced by SCO. The study assessed the effects of ethanol extract from *B. coccinea* (EEBC) on the cholinergic system, neuronal apoptosis, and antioxidant defenses. Quantitative RNA sequencing was conducted to elucidate the underlying mechanisms.

# Results

# Memory improvement effects of EEBC in SCO-mediated memory deficit mice

SCO was utilized to induce short-term memory loss<sup>27</sup>. Mice were orally administered EEBC for 20 days and received an intraperitoneal injection of SCO 30 min before behavioral tests (Fig. 1a). Throughout the experimental period, no animal deaths or significant changes in clinical signs were observed in any group. Normal body weight gains were observed, with no significant differences among the groups (Fig. 1b; Table 1).

To evaluate the potential of EEBC to mitigate memory dysfunction in SCO-injected mice, the passive avoidance test (PAT) and Y-maze test were conducted. In the PAT, SCO injection significantly reduced the retention latency compared with that in the normal control (NC) group, whereas EEBC administration at doses of 100 and 200 mg/kg significantly reversed the effects of SCO (Fig. 2a). Similarly, in the Y-maze test, the SCO group showed a significant decrease in the percentage of spontaneous alternations compared with that in the NC group. In contrast, the EEBC-100 and EEBC-200 groups showed a significant increase in the percentage of spontaneous alternations compared with that in the SCO group (Fig. 2b). The total number of arm entries did not show significant differences among the tested groups (Fig. 2c). Tacrine, as a positive control (PC), exhibited a significant effect on memory enhancement in both the PAT and Y-maze test (Fig. 2b and c).

# Effects of EEBC on the cholinergic system in SCO-mediated memory deficit mice

The cholinergic system plays an essential role in memory formation<sup>2,3</sup>. As shown in Fig. 3a and b, the SCO group had markedly decreased ACh levels and increased AChE activity compared with those in the NC group. In contrast, EEBC at doses of 100 and 200 mg/kg significantly mitigated the SCO-medicated cholinergic dysfunction. Tacrine administration significantly reversed the effects of SCO on the cholinergic system in the PC group.

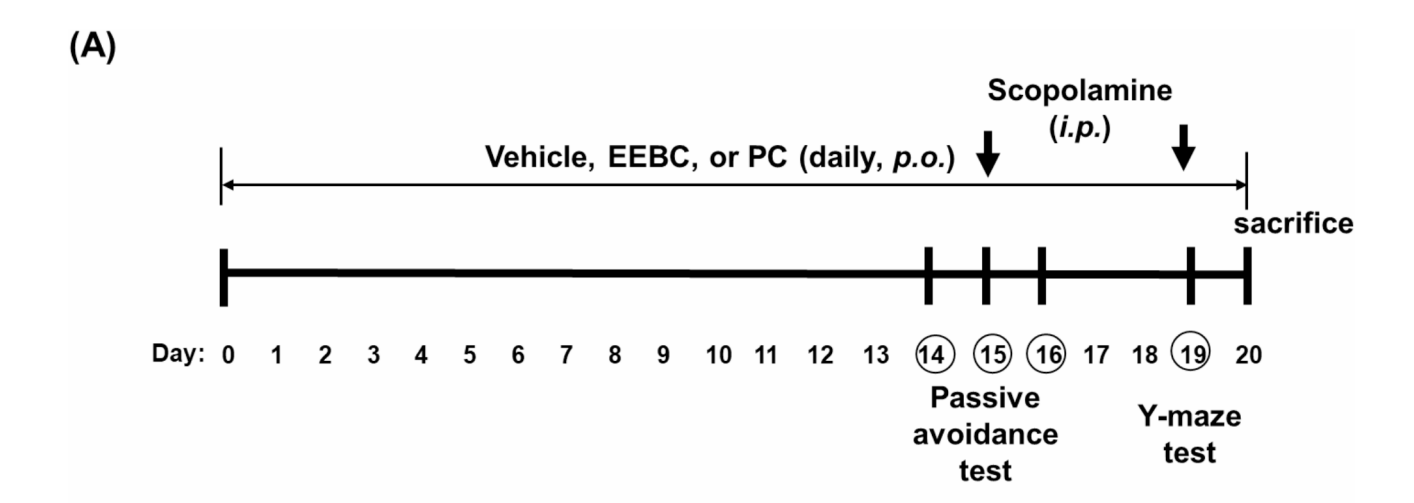
### Neuroprotective effects of EEBC in SCO-mediated memory deficit mice

To investigate the protective effects of EEBC against neuronal damage, histological analysis using Nissl staining was conducted to assess changes in cell morphology in brain tissues. SCO treatment induced morphological alternations, such as shrinkage and injury, whereas EEBC or tacrine (PC) administration considerably inhibited neuronal damage mediated by SCO injection (Fig. 4a). Additionally, SCO injection significantly reduced the number of neuronal cells in the Cornu ammonis (CA)1 and cortex areas compared with the NC group. In contrast, EEBC treatment (100 or 200 mg/kg) significantly increased the number of Nissl-positive cells compared with the SCO group (Fig. 4b,c). To further validate the neuroprotective effects of EEBC, immunohistochemistry was conducted to assess the expression of neuronal nuclei (NeuN), a neuronal marker, in hippocampal and cortical tissues. Consistent with the Nissl staining results, EEBC-treated mice that had been injected with SCO demonstrated a significant increase in NeuN-positive cells in the CA1, CA2, and cortex compared with mice that were only injected with SCO (Fig. 5a–d).

# Antiapoptotic effects of EEBC in SCO-mediated memory deficit mice

Accumulating evidence demonstrates that the cholinergic system is closely associated with the apoptotic pathway in neuronal cell death<sup>28,29</sup>. Thus, the antiapoptotic effects of EEBC were examined in mice with SCO-induced memory impairment. In the terminal deoxynucleotidyl transferase dUTP nick end labeling (TUNEL) assay, which detects apoptotic DNA fragmentation<sup>30</sup>, SCO injection significantly increased the number of TUNEL-positive cells compared with the NC group in both the hippocampus and cortex. In contrast, EEBC administration at 100 or 200 mg/kg resulted in a notable reduction in TUNEL-stained cells compared with SCO treatment. The PC, tacrine, had an inhibitory effect on SCO-induced apoptotic cell death (Fig. 6a–c).

To further verify the antiapoptotic effects of EEBC against SCO stimulation, immunoblotting was used to assess the expression of apoptosis-related factors, including Bax, Bcl2, and cleaved caspase-3, in the brain. Consistent with the TUNEL assay findings, SCO injection markedly increased the expression of Bax while decreasing that of Bcl2 compared with the NC group. In contrast, EEBC treatment reversed the SCO-induced changes in Bax and Bcl2 – members of the Bcl2 protein family. Furthermore, EEBC significantly attenuated the SCO-induced cleavage of caspase-3 (Fig. 6d–g).



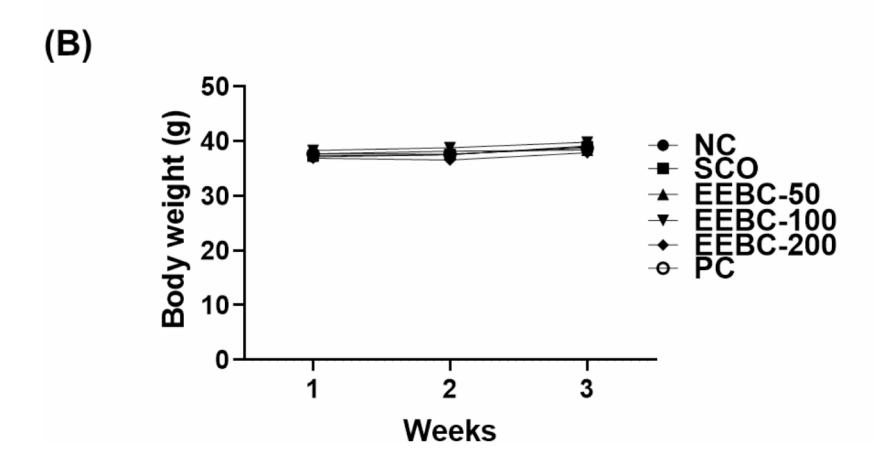


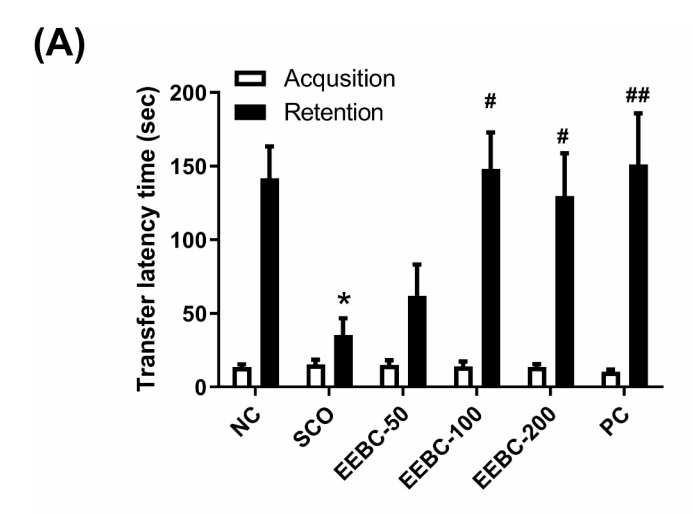
**Fig. 1.** Experimental procedures of drug administration and behavioral tests. (a) ICR mice were divided into six groups (n = 10/group): NC, normal control group; SCO, SCO-injected group; EEBC-50, group treated with 50 mg/kg of EEBC and SCO injection; EEBC-100, group treated with 100 mg/kg of EEBC and SCO injection; EEBC-200, group treated with 200 mg/kg of EEBC and SCO injection; PC, group treated with 10 mg/kg of tacrine and SCO injection. EEBC or PC were orally administered daily for 20 days. The passive avoidance task (PAT) and Y-maze test were conducted on the 14th – 16th and 19th day after SCO injection, respectively. Cognitive impairments were induced via SCO injection (1 mg/kg, i.p.) within 1 h after oral administration of EEBC. (b) Changes in body weight were measured every week after EEBC treatment. NC, normal control; SCO, scopolamine; EEBC, ethanol extract from *Bauhinia coccinea*; PC, positive control (tacrine).

		1 week	2 weeks	3 weeks
Group (n = 10/group)	NC	37.15 ± 0.24	37.54 ± 0.40	39.15 ± 0.41
	SCO	37.31 ± 0.34	37.55 ± 0.40	38.97 ± 0.52
	EEBC-50	$37.68 \pm 0.40$	38.18 ± 0.57	38.41 ± 0.61
	EEBC-100	38.31 ± 0.27	38.82 ± 0.37	39.80 ± 0.29
	EEBC-200	36.91 ± 0.49	36.56±0.73	37.90 ± 0.57
	PC	37.69 ± 0.22	37.64±0.35	38.79 ± 0.47

**Table 1.** Body weight changes of ICR mice after EEBC administration. NC, normal control group; SCO, SCO-injected group; EEBC-50, group treated with 50 mg/kg of EEBC and SCO injection; EEBC-100, group treated with 100 mg/kg of EEBC and SCO injection; EEBC-200, group treated with 200 mg/kg of EEBC and SCO injection; PC, group treated with 10 mg/kg of tacrine and SCO injection.

# Antiapoptotic effects of EEBC in H<sub>2</sub>O<sub>2</sub>-treated HT22 cells

Our previous results showed that gallic acid, a marker compound of EEBC, had an inhibitory effect on AChE activation<sup>13</sup>. To examine whether gallic acid influences the apoptosis-related proteins, Western blot analysis was performed using HT22 hippocampal cells. Cell Counting Kit (CCK) assay revealed that gallic acid had



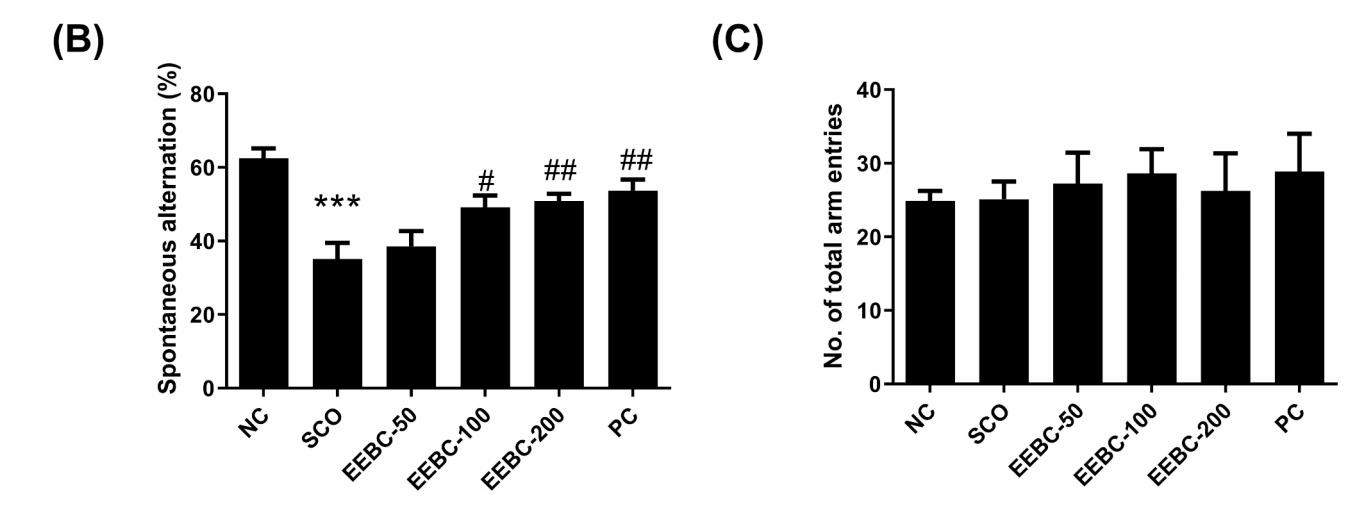


**Fig. 2.** Improvement effects of EEBC on memory impairment in a scopolamine (SCO)-induced memory deficit mouse model. (**a**) In the passive avoidance task (PAT), transfer latency time—defined as the time mice remained in the lighted compartment within 5 min—was recorded. (**b** and **c**) In the Y-maze test, each mouse was placed at the end of one arm and allowed to move freely through the maze for 8 min. The bar graphs represent the percentage of spontaneous alternation (**b**) and total number of arm entries (**c**). Data are presented as mean  $\pm$  SEM (n = 10/group).  $^*p < 0.05$  or  $^{***}p < 0.001$  vs. NC group,  $^*p < 0.05$  or  $^{***}p < 0.01$  vs. SCO group. NC, normal control; SCO, scopolamine; EEBC, ethanol extract from *Bauhinia coccinea*; PC, positive control.

no significant cytotoxicity up to 50  $\mu$ M (Fig. 7a). Neuronal cell death was induced by treatment with hydrogen peroxide (H<sub>2</sub>O<sub>2</sub>). As shown in Fig. 7b–e, gallic acid markedly reversed the H<sub>2</sub>O<sub>2</sub> effects on Bax, Bcl2, and cleaved caspase-3.

### Antioxidant effects of EEBC in SCO-mediated memory deficit mice

Oxidative stress plays a critical role in neuronal apoptosis, leading to neurodegeneration<sup>31,32</sup>. To assess the antioxidant activity of EEBC, malondialdehyde (MDA) levels and catalase activity were measured in brain tissues. The SCO group showed a significant increase in MDA levels and a decrease in catalase activity compared with the NC group. In contrast, the EEBC-100, EEBC-200, and PC groups showed a significant decrease in MDA levels, and the EEBC-200 and PC groups showed an increase in catalase activity compared with the SCO group (Fig. 8a,b).

# Molecular mechanisms of EEBC responsible for memory improvement

Transcriptome analysis was performed to explore the molecular mechanisms underlying the EEBC-induced memory improvement and neuronal protection. To observe the overall pattern of gene expression changes, we clustered 3,326 genes that showed at least 1.5-fold changes across the samples. Figure 9a shows that various genes responded to SCO and EEBC. To measure functional changes, we assessed the changes in pathway activities. The activity levels of various pathways were changed by SCO or EEBC (Fig. 9b). In particular, metabolic pathways were up-regulated by EEBC treatment. We then isolated differentially expressed genes (DEGs) in the SCO and EEBC groups using the protein–protein interaction (PPI) network. A total of 264 and 366 genes were isolated

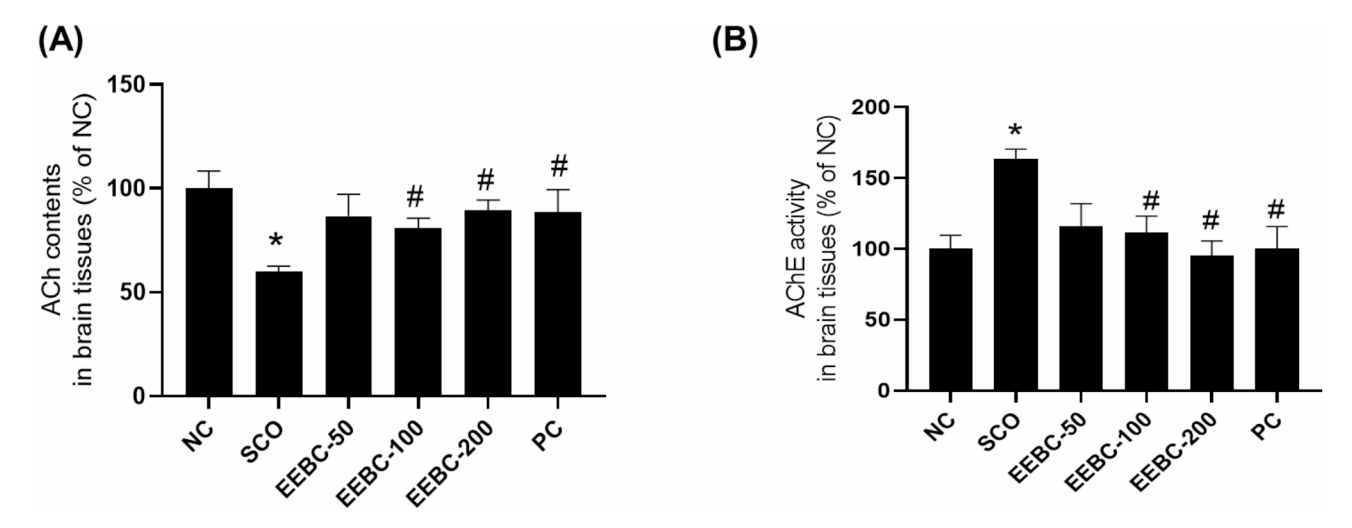


**Fig. 3.** Effects of EEBC on the cholinergic system in scopolamine (SCO)-induced memory deficit mice. Lysates from brain tissues were prepared with protein lysis buffer. ACh levels (**a**) and AChE activity (**b**) were assessed using the US Biomax ACh and AChE activity assay kits. Data are presented as mean  $\pm$  SEM (n = 3/group). \*p < 0.05 vs. NC group, \*p < 0.05 vs. SCO group. Statistical power exceeded 0.999. NC, normal control; SCO, scopolamine; EEBC, ethanol extract from *Bauhinia coccinea*; PC, positive control (tacrine).

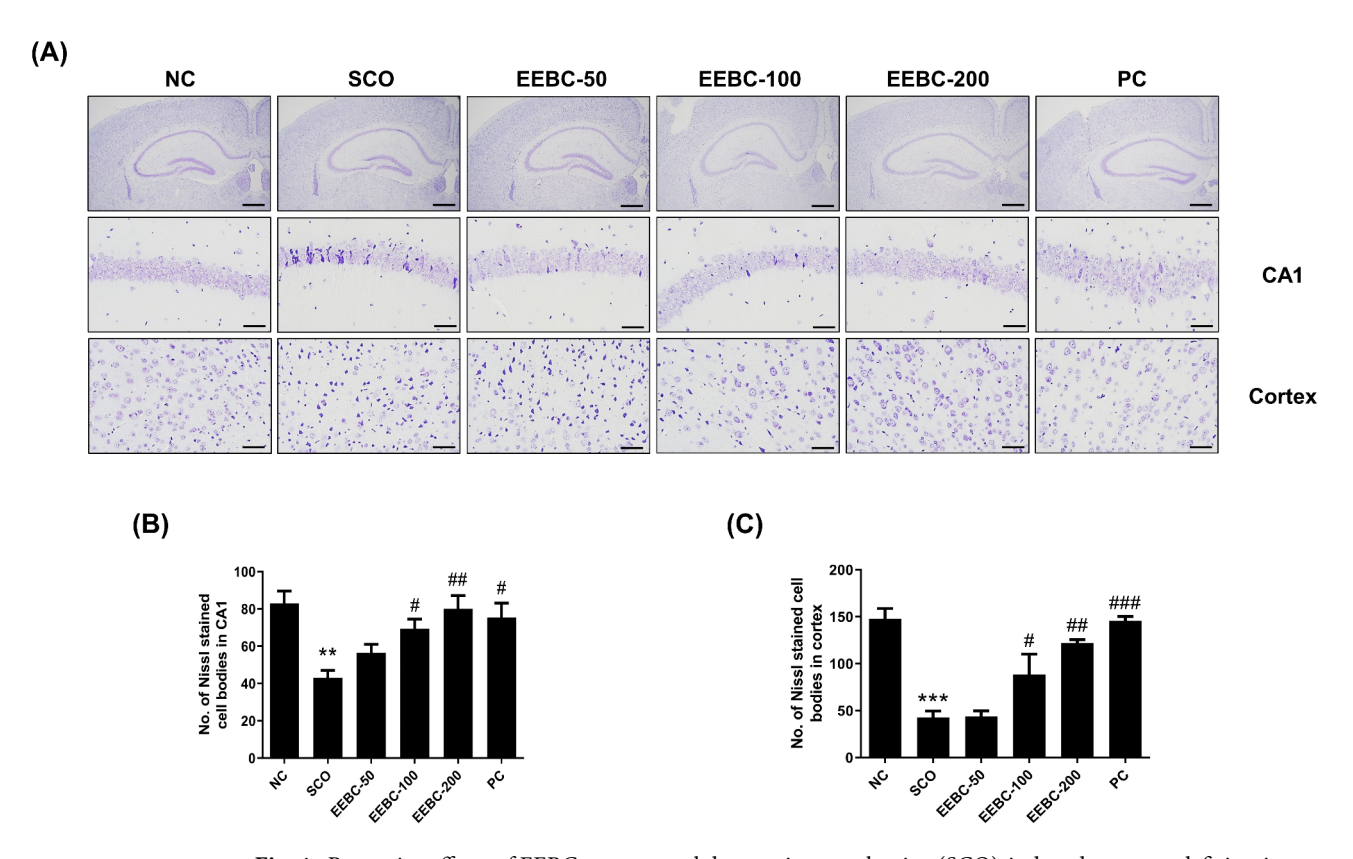


**Fig. 4.** Protective effects of EEBC on neuronal damage in scopolamine (SCO)-induced memory deficit mice. Multiple 4-μm paraffin sections of the hippocampus and cortex regions were prepared from the sacrificed mouse brains. (**a**) Nissl staining was conducted using a cresyl violet solution. Representative photomicrographs are shown at a magnification of 50× for the whole brain (upper) or 200× for CA1 (middle) and cortex (lower); scale bar, 200 μm for the whole brain or 20 μm for CA1 and cortex. (**b** and **c**) Bar graphs display the quantitative analysis of Nissl-stained cell bodies in the CA1 (**b**) and cortex (**c**). Data are presented as mean  $\pm$  SEM (n = 3/group). \*\*p < 0.01 or \*\*\*p < 0.001 vs. NC group, \*p < 0.05, \*\*p < 0.01, or \*\*\*p < 0.001 vs. SCO group. Statistical power exceeded 0.999. NC, normal control; SCO, scopolamine; EEBC, ethanol extract from *Bauhinia coccinea*; PC, positive control (tacrine); CA, cornu ammonis.

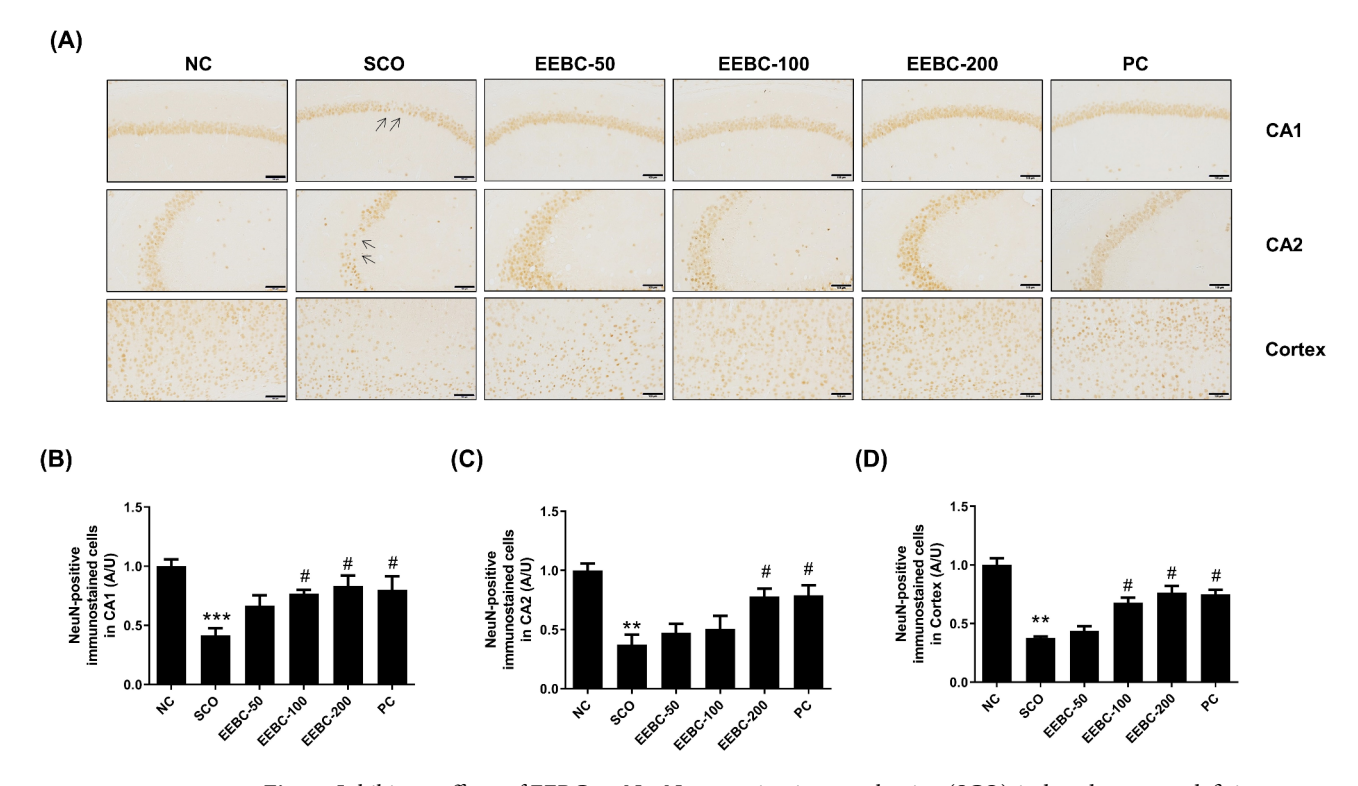


Fig. 5. Inhibitory effects of EEBC on NeuN expression in scopolamine (SCO)-induced memory deficit mice. Multiple 4- $\mu$ m paraffin sections of the hippocampus and cortex regions were prepared from the sacrificed mouse brains. (a) The expression of NeuN was immunohistochemically determined. Representative photomicrographs are shown at a magnification of 200×; scale bar, 100  $\mu$ m. (b-d) Bar graphs display the quantitative analysis of positive cells for NeuN in the CA1 (b), CA2 (c), and cortex (d). Data are presented as mean  $\pm$  SEM (n=3/group). \*\*p<0.01 or \*\*\*p<0.001 vs. NC group, \*p<0.05 vs. SCO group. Statistical power exceeded 0.999. NC, normal control; SCO, scopolamine; EEBC, ethanol extract from *Bauhinia coccinea*; PC, positive control (tacrine); CA, cornu ammonis.

as SCO group-responsive and EEBC group-responsive DEGs, respectively (empirical p-value < 0.01). The distribution of DEGs is shown as a Venn diagram in Fig. 9c. The EEBC group-responsive genes are associated with various biological functions, such as lipid metabolism processes (false discovery rate (FDR) < 0.01), as shown in Fig. 9d. Gene ontology (GO)-term network analysis also showed that these lipid metabolism processes are closely interconnected (Fig. 9e). Finally, we measured the interactions among DEGs in the PPI interaction network. Figure 9f shows that the DEGs in the SCO group directly or indirectly interacted with the DEGs in the EEBC group to form large gene clusters. These results suggest that EEBC treatment may interfere with the SCO effect at the gene level, resulting in therapeutic effects.

#### Discussion

We previously reported the in vitro anti-AD potential of an extract from B. coccinea branches<sup>13</sup>. EEBC has an inhibitory effect on major AD biomarkers, including AB aggregation and AChE activation. EEBC significantly prevented H<sub>2</sub>O<sub>2</sub>-induced cell death in hippocampal cells, indicating neuroprotective activity. EEBC also demonstrated antioxidant properties by increasing radical scavenging. Moreover, we conducted a simultaneous analysis of four marker compounds in EEBC using high-performance liquid chromatography (HPLC) for quality control. We identified (+)-catechin as the most abundant compound compared with other markers, such as ellagic acid, gallic acid, and quercitrin. Additionally, gallic acid was found to exhibit the highest inhibitory activity among the four marker compounds in the AChE activity assay, demonstrating the possibility that gallic acid is a bioactive compound of EEBC regulating the cholinergic system. In the present study, we extended our investigation to in vivo models to further validate the potential of EEBC. Our results demonstrate that EEBC effectively mitigates SCO-induced memory impairment and neuronal damage in mice by modulating the cholinergic system as well as the antiapoptotic and antioxidant pathways. Gallic acid also affected the apoptosisrelated proteins Bax, Bcl2, and caspase-3 in H<sub>2</sub>O<sub>2</sub>-treated hippocampal cells. Notably, more detailed molecular mechanisms were elucidated using the QuantSeq 3'mRNA sequencing analysis. We noticed that the memory improvement potential of EEBC is associated with lipid metabolism pathways. These findings highlight the therapeutic potential of EEBC in combating AD and related neurodegenerative conditions.

Memory loss is an early sign and symptom in individuals with or at risk of AD<sup>33,34</sup>. In animal models, behavioral tests are the most widely accepted approach for evaluating memory function<sup>35,36</sup>. Behavioral tests revealed that EEBC administration improved memory performance in SCO-injected mice, as evidenced by enhanced retention latency in the PAT and increased spontaneous alternation in the Y-maze test. SCO is a non-

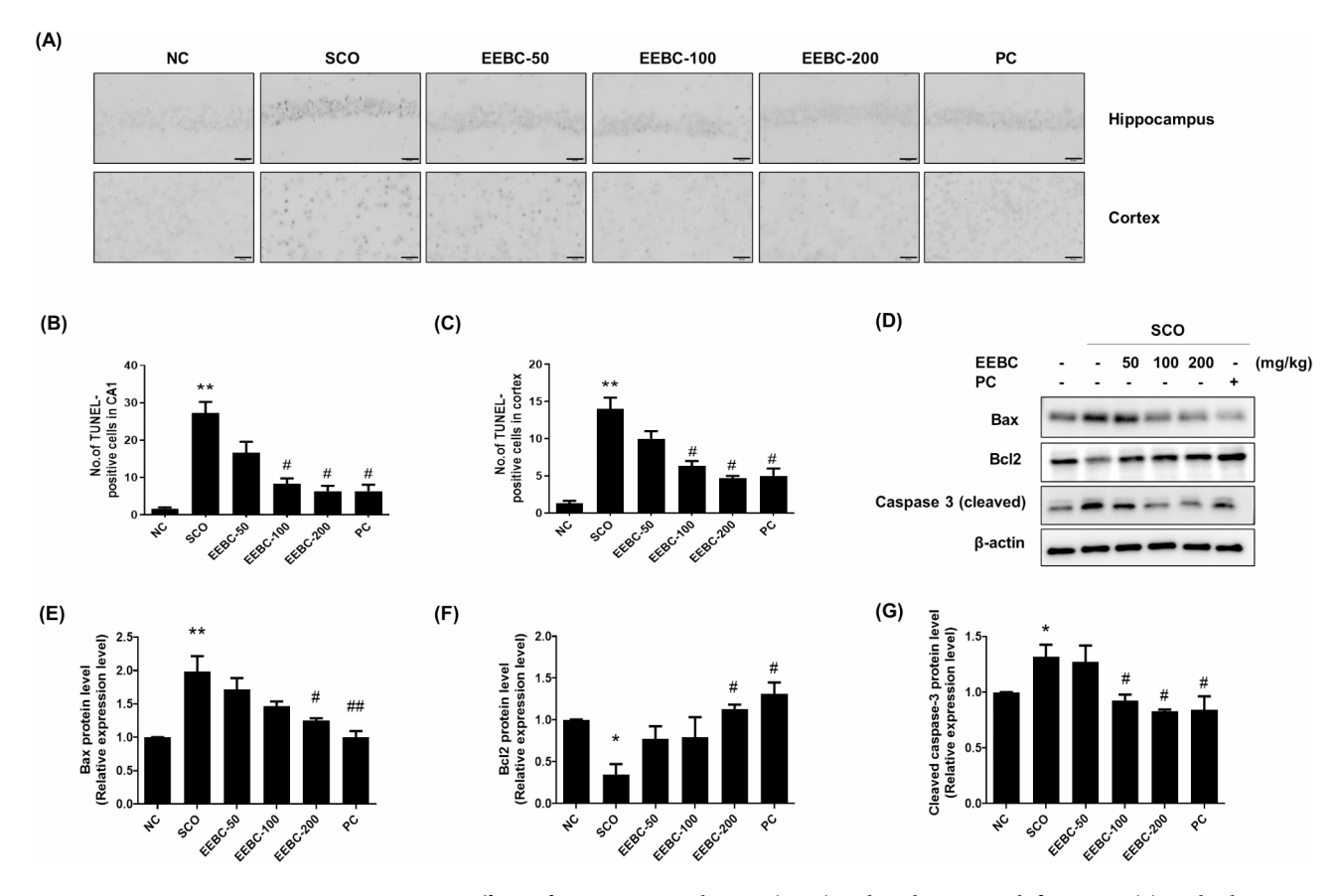


**Fig. 6.** Antiapoptotic effects of EEBC in scopolamine (SCO)-induced memory deficit mice. (a) Multiple 4-μm paraffin sections of the hippocampus and cortex regions were prepared from the sacrificed mouse brains. TUNEL staining was performed using an InSitu Cell Death Detection AP Kit (Roche Diagnostics, Mannheim, Germany). Apoptotic cells were visualized with nitro blue tetrazolium and 5-bromo-4-chloro-3-indolyl-phosphate (NBT/BCIP-AP, purple). Counterstaining for nuclei was performed with Fast-red. Representative photomicrographs are shown at a magnification of 200×; scale bar, 50 μm. (b and c) Bar graphs display the quantitative analysis of the apoptotic cells in the hippocampus (b) and cortex (c). (d) Whole brain tissues were lysed and subjected to Western blotting with anti-Bax, Bcl2, and cleaved caspase-3 antibodies. Full uncut blots are shown in Supplementary Fig. 1. (e-g) Bar graphs display the quantitative analysis of protein expression of Bax (e), Bcl2 (f), and cleaved caspase-3 (g). Expression levels were normalized to β-actin. Western blotting was repeated three times for each protein. Data are presented as mean ± SEM (n=3/group).  $^*p$ <0.05 or  $^**p$ <0.01 vs. NC group,  $^*p$ <0.05 or  $^**p$ <0.01 vs. SCO group. Statistical power exceeded 0.999. NC, normal control; SCO, scopolamine; EEBC, ethanol extract from *Bauhinia coccinea*; PC, positive control (tacrine); TUNEL, terminal deoxynucleotidyl transferase dUTP nick end labeling.

selective antagonist of muscarinic receptors that inhibits short-term memory acquisition in human and animal models<sup>28</sup>. The cholinergic hypothesis is the earliest theory on the pathogenesis of AD<sup>37</sup>. ACh is a neurotransmitter involved in learning and memory, influenced by the central cholinergic nervous system<sup>38–40</sup>. AChE, an essential enzyme responsible for ACh degradation, prevents postsynaptic signal transmission<sup>41</sup>. Patients with AD have reduced cholinergic neurons in the brain<sup>42,43</sup>. Therefore, restoring the cholinergic system in the damaged brain is a crucial therapy aspect for patients with AD. In the present study, EEBC treatment mitigated these effects by preserving ACh levels and reducing AChE activity in the hippocampal and cortical regions of SCO-injected mice, consistent with previous in vitro findings<sup>13</sup>. These findings suggest that EEBC may restore cholinergic neurotransmission, essential for memory and learning, thereby reversing SCO-induced cognitive deficits.

Neuronal death is a hallmark of neurodegenerative diseases 44,45. In the pathogenesis of AD, neuronal loss begins in the pre-clinical stage and progresses through mild cognitive impairment to AD, ultimately contributing to memory dysfunction 46,47. Histological analyses through Nissl staining and NeuN immunohistochemistry revealed that EEBC protects neuronal integrity against SCO-induced damage. EEBC treatment significantly increased the number of Nissl- and NeuN-positive cells in the hippocampus and cortex, indicating its neuroprotective capabilities. The reduction in apoptotic cells, as shown by the TUNEL assay, further substantiates the antiapoptotic effects of EEBC. Western blot analysis provided molecular evidence of these protective effects, showing that EEBC modulates apoptosis-related protein expression. EEBC treatment reversed the SCO-induced upregulation of proapoptotic Bax and downregulation of antiapoptotic Bcl2, and decreased the activation of cleaved caspase-3. We also examined the effects of gallic acid—a candidate bioactive compound of EEBC—on

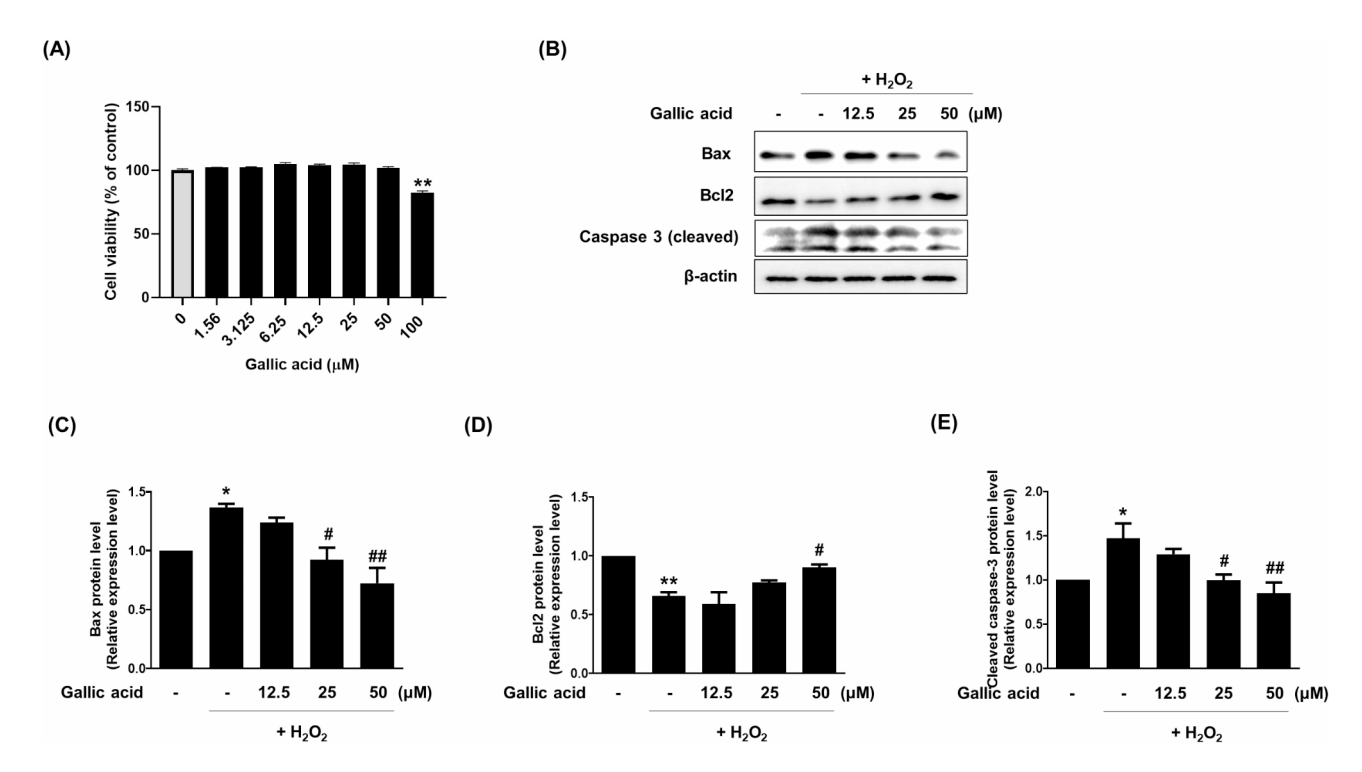
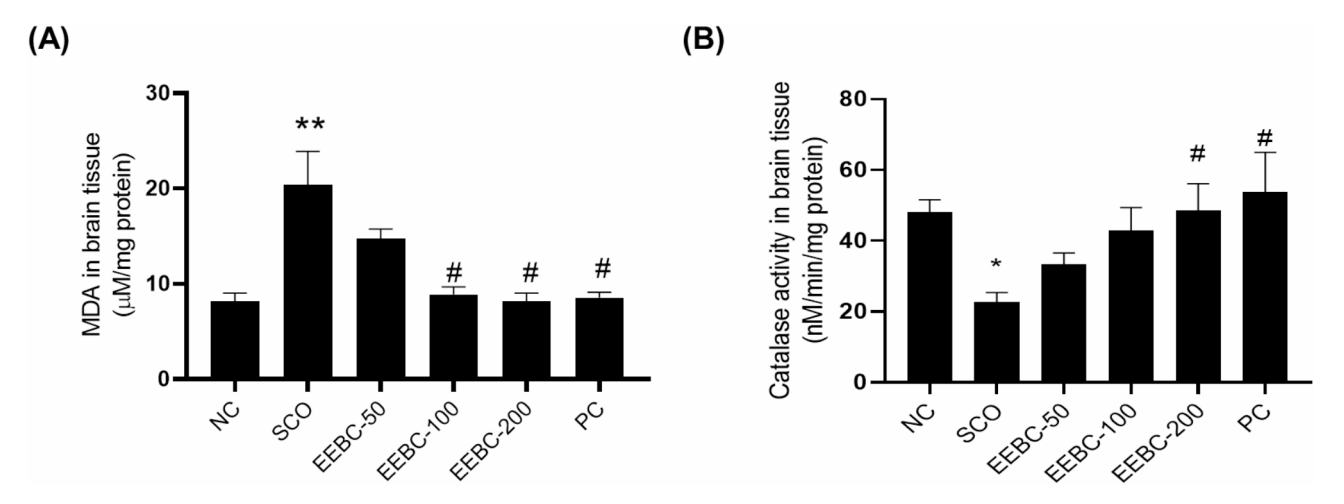
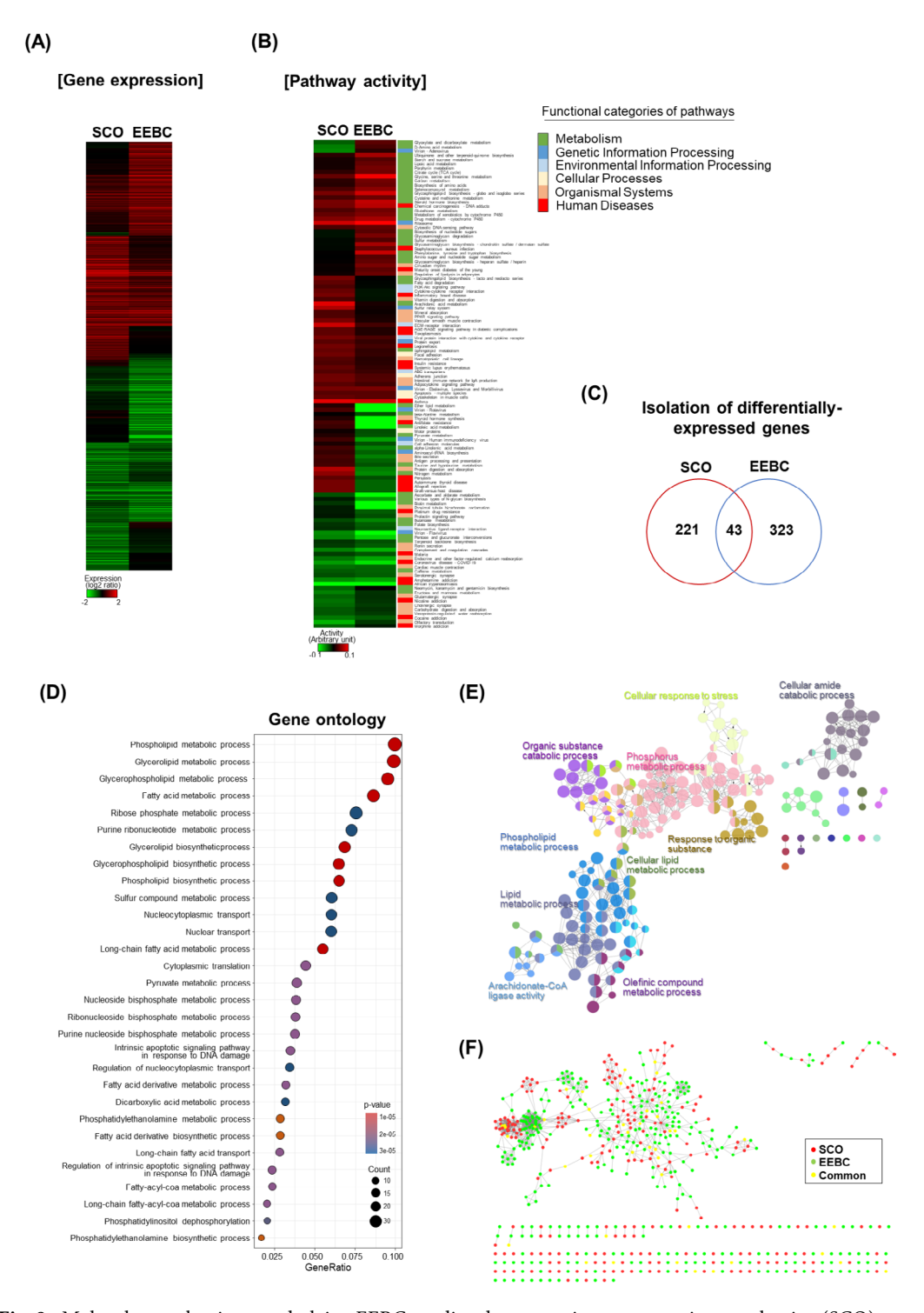


Fig. 7. Antiapoptotic effects of gallic acid in  $H_2O_2$ -treated HT22 hippocampal cells. (a) Hippocampal cells were seeded in 96-well plates and treated with gallic acid (at concentrations of 0, 1.56, 3.125, 6.25, 12.5, 25, 50, or 100 μM) for 24 h. Cell viability was measured using the CCK-8 assay. (b) Cells were treated with  $H_2O_2$  (250 μM) in the absence or presence of EEBC (12.5, 25, or 50 μM). The cells were lysed and subjected to Western blotting with anti-Bax, Bcl2, and cleaved caspase-3 antibodies. Full uncut blots are shown in Supplementary Fig. 2. (c-e) Bar graphs display the quantitative analysis of Bax (c), Bcl2 (d), and cleaved caspase-3 (e) protein expression. Expression levels were normalized to β-actin. Western blotting was repeated three times for each protein. Data are presented as mean ± SEM (n=3/group). \*p<0.05 or \*\*p<0.01 vs. untreated control, \*p<0.05 or \*\*p<0.01 vs.  $H_2O_2$ -treated cells. Statistical power exceeded 0.999.  $H_2O_2$ , hydrogen peroxide; EEBC, ethanol extract from \*Bauhinia coccinea\*.



**Fig. 8.** Antioxidant effects of EEBC in scopolamine (SCO)-induced memory deficit mice. Lysates from brain tissues were prepared with protein lysis buffer. (a) Intracellular levels of malondialdehyde (MDA) were evaluated using the MDA assay kit (Cayman, Ann Arbor, MI). (b) Catalase enzyme activity was measured using the Catalase activity kit (Cayman). The absorbance of the samples was read at 540 nm. Data are presented as mean  $\pm$  SEM (n = 4/group).  $^*p < 0.05$  or  $^{**}p < 0.01$  vs. NC group,  $^*p < 0.05$  vs. SCO group. Statistical power exceeded 0.999. NC, normal control; SCO, scopolamine; EEBC, ethanol extract from *Bauhinia coccinea*; PC, positive control (tacrine).



**Fig. 9.** Molecular mechanisms underlying EEBC-mediated memory improvement in scopolamine (SCO)-induced memory deficit mice. (a) Genes (3,326) showing at least 1.5-fold changes across samples were hierarchically clustered based on similarity in expression levels. The rows and columns represent the gene and sample, respectively. The expression level of the gene is color-coded, as the bottom scale bar indicates; red and green represent high and low gene expression ratios, respectively. (b) Pathway activity levels were measured and clustered. The activity level is indicated in color, as the bottom scale bar indicates. Red and green represent high and low levels of pathway activity, respectively. The six functional categories of each pathway are also displayed in color, as shown in the bar on the right. (c) DEGs isolated from each sample were compared using a Venn diagram. (d) A list of enriched gene ontology (GO) terms (p<0.001) associated with EEBC-responsive genes is shown. (e) GO terms (p<0.001) associated with EEBC-responsive genes are interconnected in the network. Representative ontology terms are indicated. (f) The distribution of DEGs in the PPI network was measured; DEGs by SCO or EEBC treatment are shown in red or green, respectively. Common DEGs are shown in yellow. SCO, scopolamine; EEBC, ethanol extract from *Bauhinia coccinea*.

apoptosis-related proteins. Consistent with previous reports<sup>48,49</sup>, gallic acid treatment significantly reversed the expression of Bax, Bcl2, and caspase-3 in oxidative stress-damaged neuronal cells. These findings indicate that EEBC attenuates neuronal apoptosis by regulating the intrinsic apoptotic pathway, potentially contributing to the preservation of cognitive functions.

Oxidative stress has neurotoxic potential and plays a critical role in neurodegeneration  $^{50}$ . In the pathogenesis of AD, an abnormal deposition of A $\beta$  aggregates—resulting from an increase in free radicals or impaired antioxidant defenses—induces oxidative stress and neurotoxicity in the brain  $^{51}$ . As mentioned above, we previously proposed that EEBC has a protective effect against  $H_2O_2$ -induced cell death in neuronal cells, as well as significant free radical scavenging activity  $^{13}$ . The present study demonstrates that EEBC significantly reduced MDA levels and increased catalase activity in the brains of SCO-administered mice, indicating robust antioxidant activity. These findings align with the neuroprotective effects observed in various other plant extracts, such as those from *M. esculenta*  $^6$ , *Thymus daenensis*  $^{52}$ , *Emilia coccinea*  $^{53}$ , and *Drynaria quercifolia*  $^{54}$ , which have been shown to mitigate memory impairment and oxidative stress in similar models. These natural extracts are multicomponent and multi-target substances. Therefore, they should be considered more valuable and important drug candidates for targeting the multifarious mechanisms of AD compared with single chemicals.

We finally elucidated the molecular mechanisms by which EEBC modulates memory improvement. Transcriptome analysis revealed that lipid metabolic processes, such as those involving phospholipids, glycerolipids, and glycerophospholipids, were highly enriched in SCO-treated mice with EEBC administration; this suggests the importance of lipid metabolism in memory improvement exerted by EEBC. The brain is rich in lipids, including phospholipids, cholesterol, and sphingolipids<sup>55</sup>. In the brain, lipid metabolism dysregulation resulting in lipid peroxidation and lipid profile alternations is associated with neurodegenerative disease, such as AD<sup>56</sup>. Thus, specifically targeting lipid metabolism may open up new avenues for developing AD drugs to improve cognitive function in which EEBC may be a potent candidate.

In our animal study, we used tacrine as a PC. Tacrine is an AChE inhibitor approved by the U.S. FDA for AD treatment<sup>57</sup>, although it was discontinued owing to safety issues<sup>58</sup>. Previous preclinical and clinical studies suggested beneficial effects on cognitive and memory function from tacrine use<sup>59,60</sup>. Tacrine also exerts a neuroprotective effect via antiapoptotic regulation and antioxidant activity<sup>61</sup>. As mentioned, EEBC is a multicompound complex whereas tacrine is a small molecule. Positive interaction among EEBC components may synergistically promote pharmacological activity against AD. We observed that EEBC had considerably similar effects to those of tacrine on memory improvement, neuroprotection, and antiapoptosis activity. Moreover, antioxidation assays revealed EEBC superiority, compared with tacrine, in improving AD-related symptoms. This may render EEBC a more attractive drug than tacrine.

Further research is needed to elucidate the detailed molecular pathways involved in EEBC's neuroprotective effects associated with lipid metabolism and to evaluate its efficacy in other models of neurodegeneration. Additionally, the safety and pharmacokinetics of EEBC should be thoroughly investigated to pave the way for potential clinical applications. Preclinical toxicity tests will be performed according to the OECD Good Laboratory Practice. We will also consider clinical trials to validate the safety and efficacy guidelines for EEBC in a future study.

In conclusion, the present study provides compelling evidence that *B. coccinea* extract ameliorates SCO-induced memory impairment through cholinergic enhancement, antiapoptotic activity, antioxidative defense, and lipid metabolism. Our findings suggest that EEBC is a promising therapeutic candidate for AD, targeting multiple pathways involved in the pathogenesis of the disease. EEBC's ability to enhance cholinergic function, protect against neuronal apoptosis, and exert antioxidant effects underscores its potential as a multifaceted treatment strategy for AD.

# Methods

# Plant materials and EEBC preparation

*B. coccinea* branches were provided by the Korean Seed Association and identified by Prof. Joo-Hwan Kim (Gachon University, Seongnam, South Korea). A voucher specimen (No. SCD-A-115) was deposited at the Herbarium in the Korean Medicine Convergence Research Division, Korea Institute of Oriental Medicine (Daejeon, South Korea).

The dried samples were cut into small pieces and extracted three times with  $10\times$  the volume of 70% aqueous ethanol for 1 week. The extracted solution was filtered through Whatman filter paper (pore size, 5 µm) and concentrated using a rotary evaporator (EYELA N-1000, Rikakikai Co., Tokyo, Japan) under vacuum. The yield of EEBC was 18.86%. Quality control data for EEBC using HPLC are reported in our previous paper<sup>13</sup>.

# Animals and drug treatments

The experiments were performed according to the National Institutes of Health (NIH) Guide for the Care and Use of Laboratory Animals and approved by the Korea Institute of Oriental Medicine Institutional Animal Care and Use Committee (IACUC Approval No.18 – 002). ICR mice (7 weeks old, male, 25–28 g) were obtained from the Daehan Biolink (Cheongju, South Korea) and acclimatized for 1 week before being fed standard food and water *ad libitum*. Mice were housed under controlled conditions: a 12-h light/dark cycle,  $22\pm2$  °C, 55% humidity. Sixty mice were randomly divided into six groups (n=10/group): NC, normal control; SCO, SCO-injected; EEBC-50, treated with 50 mg/kg EEBC and SCO injection; EEBC-100, treated with 100 mg/kg EEBC and SCO injection; and PC, treated with 10 mg/kg tacrine and SCO injection. Researchers conducted all animal experiments in a blinded manner.

EEBC was dissolved in distilled water at doses of 50, 100, or 200 mg/kg administered daily by gastric gavage for 3 weeks. Tacrine (USP, Rockville, MD) was administered to the PC group. Distilled water was used as a vehicle control. Mice were intraperitoneally injected with SCO (1 mg/kg) within 60 min after the oral administration of

EEBC or PC to induce memory impairment, except for mice in the NC group, which received saline. Behavioral tests were conducted 30 min after SCO injection. The animal study procedures were performed according to the ARRIVE guidelines.

# PAT

The PAT was conducted using the Gemini Avoidance system (San Diego Instruments, San Diego, CA). The system consists of two identical compartments, one lighted and one darkened, separated by an automated door and featuring an electrifiable grid floor. During the acquisition phase, mice were allowed to familiarize themselves with the environment in the lighted compartment for 25 s before crossing to the darkened compartment. The door automatically opened, and they received a mild electrical shock at 0.3 mA for 3 s. During the retention phase, mice were placed back in the lighted compartment. The retention time was recorded to measure the latency time required for mice to move from the lighted to the darkened compartment. If mice did not move to the darkened compartment within 5 min, the latency time was recorded as 300 s. No physiological defects (i.e., motor deficits) or intrinsic cognitive impairments were detected in any group before SCO injection.

#### Y-maze test

The Y-maze was positioned with its three arms at equal angles (length, 35 cm; height, 15 cm; width, 7 cm). Each mouse was placed in one arm and allowed to spontaneously explore the maze for 8 min. The number of spontaneous alternations was assessed using the EthoVision XT tracking system (Noldus Information Tech, Wageningen, Netherlands). Spontaneous alternation (%) was calculated using the equation reported below. Spontaneous alternation (%) = [(number of alternations) / (total number of arm entries-2)] × 100.

At the end of the experiment, mice were sacrificed under deep anesthesia by intraperitoneal injection with Avertin – an agent mainly composed of 2,2,2-tribromoethanol (T48402, Sigma-Aldrich, St. Louis, MO). Three mouse brains from each group were perfused intracardially with phosphate-buffered saline (pH 7.4), fixed in 4% paraformaldehyde, embedded in paraffin, and 4-µm-thick sections were prepared.

# Histological staining

For Nissl staining, deparaffinized and hydrated slides were immersed in 1% cresyl violet solution for 1 min to stain the Nissl substance, followed by washing with tap water. For TUNEL staining, the In Situ Cell Death Detection AP Kit (11684809910, Roche Diagnostics, Mannheim, Germany) was used according to the manufacturer's protocol. Apoptotic cells were stained with nitro blue tetrazolium and 5-bromo-4-chloro-3-indolyl-phosphate (11681451001, NBT/BCIP, Roche Diagnostics) solution. Sections stained by both Nissl and TUNEL methods were visualized using an Olympus DP71 microscope (Tokyo, Japan) at 400× magnification. The images were analyzed and the stained cells were quantified using ImageJ software (NIH, Bethesda, MD).

# Immunohistochemistry for NeuN expression

Histology slide preparation of brain tissues

The slides were deparaffinized and hydrated with xylene and sequential ethanol solutions. Endogenous peroxidase activity was quenched with 0.3%  $\rm H_2O_2$  in methanol, and antigen retrieval was performed by boiling in citrate buffer (pH 6.0). Slides were blocked with horse serum for 1 h at 37°C and probed overnight at 4°C with anti-NeuN antibody (ab104225, Abcam, Cambridge, UK). Subsequently, slides were incubated with labeled streptavidin–biotin for 30 min and developed using diaminobenzidine tetrahydrochloride (DAB; SK-4105, Vector Laboratories, Burlingame, CA). Mounted slides were captured at 400× magnification using an Olympus DP71 microscope. The images were analyzed and the stained cells quantified using ImageJ software.

#### ACh level and AChE activity assays

ACh levels and AChE activity in the mouse brain were measured using commercial assay kits (BM-ACH-100, US Biomax, Denwood, MD) according to the manufacturer's instructions. The absorbance of the reaction mixture was measured at 570 nm using a Benchmark Plus spectrophotometer (Bio-Rad, Hercules, CA).

# MDA and catalase activity assays

Intracellular levels of MDA (10009055, Cayman, Ann Arbor, MI) and catalase activity (Cayman) were measured in brain tissues according to the manufacturer's protocol. The absorbance of the reaction mixture was measured at 540 nm using a Benchmark Plus microplate reader.

#### Cell culture and treatment

HT22 mouse hippocampal neuronal cells were maintained in Dulbecco's Modified Eagle's Medium (Hyclone/ Thermo, Rockford, IL), containing 10% fetal bovine serum and penicillin/streptomycin, at 37  $^{\circ}$ C with a 5% CO<sub>2</sub> atmosphere. The cells were co-treated with EEBC and H<sub>2</sub>O<sub>2</sub>.

#### Cell viability assay

Cell viability was evaluated using the CCK-8 (Dojindo, Kumamoto, Japan). HT22 cells were seeded into 96-well microplates at a density of  $5\times10^3$  cells/well and treated with EEBC for 24 h. After incubating with the CCK-8 solution, the absorbance was assessed at 450 nm using an Epoch microplate spectrophotometer (BioTek Instruments, Inc., Winooski, VT). Cell viability (% of control) was estimated using the following equation:

$$\label{eq:cellval} \text{Cell viability (\% of control)} = \frac{\text{Optical density in EEBC} - \text{treated cells}}{\text{Optical density in untreated cells}} \ \times \ 100$$

# Western blot analysis

CelLytic MT Cell Lysis Reagent (Sigma-Aldrich, St. Louis, MO) and radioimmunoprecipitation buffer (pH 7.5) containing phosphatase and protease inhibitors (Pierce Biotechnology, Rockford, IL) were used to isolate proteins from cells and brain tissues, respectively. Proteins were separated on 4–20% gradient polyacrylamide gels (Thermo Fisher Scientific, Waltham, MA) and transferred to polyvinylidene difluoride membranes. The membranes were blocked with 5% non-fat milk and then incubated with antibodies against Bax (14796 S), Bcl2 (2780 S), cleaved caspase-3 (9664 S) (Cell Signaling Technology, Danvers, MA, 1:1000 dilution), and  $\beta$ -actin (SC-376421) (Santa Cruz Biotechnology, Dallas, TX, 1:3000 dilution). Subsequently, the membranes were incubated with secondary antibodies conjugated with horseradish peroxidase and developed using a SuperSignal ECL solution (34577, Amersham Bioscience, Piscataway, NJ). Protein bands were detected using a Las-4000 MINI ChemiDox imaging analyzer (Fuji Photo, Tokyo, Japan).

### **RNA** isolation

Total RNA was extracted from brain tissues using TRIzol reagent, according to the manufacturer's instructions (Invitrogen, Carlsbad, CA). RNA quality was assessed using the Agilent TapeStation 4000 system (Agilent Technologies, Amstelveen, Netherlands). RNA samples with integrity>7.0 were included in the QuantSeq Analysis.

# Library preparation and sequencing for QuantSeq analysis

Library construction was performed using QuantSeq 3' mRNA-Seq Library Prep Kit (Lexogen, Inc., Austria). Each total RNA was prepared and an oligo-dT primer containing an Illumina-compatible sequence at the 5'-end was hybridized to the RNA and reverse transcription was performed. After RNA template degradation, second strand synthesis was initiated by a random primer containing an Illumina-compatible linker sequence at its 5'-end. The double-stranded library was purified using magnetic beads to remove all reaction components. The library was amplified to add the complete adapter sequences required for cluster generation. The finished library was purified from the PCR components. High-throughput sequencing was performed as single-end 75 sequencing using NextSeq 550 (Illumina, Inc., San Diego, CA).

# QuantSeq data analysis

QuantSeq 3' mRNA-Seq reads were performed as previously described<sup>62</sup>. Gene expression profiles were measured by hierarchically clustering genes based on similarity in expression levels using Gene Cluster 3.0 and visualized using Java TreeView<sup>63</sup>. Functional enrichment analysis using a group of genes can provide a simplified characterization of functional changes occurring in a sample. In this study, we measured functional changes at the pathway level; that is, pathway activity, using the expression levels of all genes rather than a few selected genes. Briefly, after log-transforming the expression ratio of each gene relative to that of the control group, the activity level was calculated by linearly adding the ratios of all the genes included in each pathway. A weight of -1 was assigned to genes (or proteins) that inhibit the direction of signal transmission in the pathway to reflect the inhibitory effect. The final pathway activity value was calculated by dividing the measured value by the number of genes in the pathway. Statistical significance of the activity value was empirically determined after 1,000 random permutations of the phenotypes<sup>64</sup>. Information such as genes contained in individual pathways and higher functional categories of pathways was obtained from the KEGG database (http://www.genome.jp/ke gg). All analytical processes were performed using R (version 4.3.0).

# Isolation of differentially-expressed genes

DEGs from each sample were isolated using a module-based approach in an integrated interactome with the igraph R package (version 1.2.6)65. Specifically, the gene module was composed of individual genes and their neighboring genes that interacted with each other in the PPI network obtained from the Biogrid database (version 4.4.210)66. The average and standard deviation of each module were measured by comparing the expression values of the genes with those of the control group within the module. The statistical significance of the values measured in the original module was determined using empirical methods. That is, the same measurement was repeated 1,000 times using a random module of the same size as the original module, and the measured values were then compared with the original value. We then isolated the core genes showing differential expression patterns (empirical p-value < 0.01). To isolate core genes showing differential expression between samples, the correlation coefficient between the expression levels of genes included in the modules of each sample was measured in addition to the mean and SD. As in the case of individual samples, the statistical significance of the gene was measured empirically through 1,000 iterations using random genes from each sample. As a result, genes with an empirical p-value < 0.01 were selected as core-differential genes. To isolate genes showing differential expression between the hippocampus and cortex under normal conditions, we performed the same process using the ratio of expression in the hippocampus versus the cortex. All processes were implemented in R (version 4.3.0).

# Statistical analysis

Data are expressed as mean  $\pm$  standard error of the mean. Data were analyzed using one-way analysis of variance followed by Dunnett's multiple comparisons test. Statistical significance was set at p < 0.05. All analyses were conducted using GraphPad Prism 9.1 (GraphPad Software, San Diego, CA).

# Data availability

Data will be made available from the corresponding author (sjijeong@kiom.re.kr) on reasonable request.

Received: 23 August 2024; Accepted: 24 January 2025

Published online: 03 February 2025

### References

- 1. Ribeiro, F. M. Understanding brain diseases: From receptor dysregulation to neurodegeneration, neuroinflammation and memory impairment. *Curr. Neuropharmacol.* **21**, 162–163 (2023).
- 2. Gedankien, T. et al. Acetylcholine modulates the temporal dynamics of human theta oscillations during memory. *Nat. Commun.* **14**, 5283 (2023).
- 3. Chen, Z. R., Huang, J. B., Yang, S. L. & Hong, F. F. Role of cholinergic signaling in Alzheimer's disease. Molecules 27, 1816 (2022).
- 4. Thompson, K. J. & Tobin, A. B. Crosstalk between the M1 muscarinic acetylcholine receptor and the endocannabinoid system: A relevance for Alzheimer's disease. *Cell. Signal.* **70**, 109545 (2020).
- 5. Mohammad, D., Chan, P., Bradley, J., Lanctôt, K. & Herrmann, N. Acetylcholinesterase inhibitors for treating dementia symptoms—a safety evaluation. *Expert Opin. Drug Saf.* 16, 1009–1019 (2017).
- Carrazoni, G. S. et al. Supplementation with Manihot esculenta Crantz (Cassava) leaves' extract prevents recognition memory deficits and hippocampal antioxidant dysfunction induced by amyloid-β. Nutr. Neurosci. 10, 1–9 (2023).
- Ibrahim, W. W. et al. Neuroprotective potential of Erigeron bonariensis ethanolic extract against ovariectomized/D-galactose-induced memory impairments in female rats in relation to its metabolite fingerprint as revealed using UPLC/MS. Inflammopharmacology 32, 1091–1112 (2024).
- 8. Lim, H. S. et al. *Annona atemoya* leaf extract ameliorates cognitive impairment in amyloid-β injected Alzheimer's disease-like mouse model. *Exp. Biol. Med. (Maywood).* **244**, 1665–1679 (2019).
- Sohn, E. et al. ElaeGlabraglabra f. oxyphylla attenuates scopolamine-induced learning and memory impairments in mice by improving cholinergic transmission via activation of CREB/NGF signaling. Nutrients 11, 1205 (2019).
- Sohn, E., Kim, Y. J., Kim, J. H. & Jeong, S. J. Ficus erecta TLeavesleaves ameliorate cognitive deficit and neuronal damage in a mouse model of amyloid-β-induced Alzheimer's disease. Front. Pharmacol. 12, 607403 (2021).
- 11. Balkrishna, Å. et al. Exploring the safety, efficacy, and bioactivity of herbal medicines: bridging traditional wisdom and modern science in healthcare. Future Integr. Med. 3, 35–49 (2024).
- Heydari, M., Rauf, A., Thiruvengadam, M., Chen, X. & Hashempur, M. H. Editorial: clinical safety of natural products, an evidence-based approach. Front. Pharmacol. 13, 960556 (2022).
- Kim, Y. J. et al. Simultaneous quantification of four marker compounds in *Bauhinia coccinea* extract and their potential inhibitory effects on Alzheimer's disease biomarkers. *Plants (Basel)*. 10, 702 (2021).
- Kumar, S., Kumar, R., Gupta, Y. K. & Singh, S. In vivo anti-arthritic activity of Bauhinia purpurea Linn. Bark extract. Indian J. Pharmacol. 51, 25–30 (2019).
- 15. Pinafo, M. S. et al. Effects of *Bauhinia forficata* on glycaemia, lipid profile, hepatic glycogen content and oxidative stress in rats exposed to bisphenol A. *Toxicol. Rep.* 6, 244–252 (2019).
- 16. Jian, J., Xuan, F., Qin, F. & Huang, R. The antioxidant, anti-inflammatory and anti-apoptotic activities of the *Bauhinia championii* flavone are connected with protection against myocardial ischemia/reperfusion injury. *Cell. Physiol. Biochem.* 38, 1365–1375 (2016)
- 17. Annapurna, A., Vishala, T. C., Bitra, V. R., Rapaka, D. & Shaik, A. Cerebroprotective actions of *Triticum aestivum* Linn powder and *Bauhinia purpurea* flower powder in surgically induced cerebral infraction in rats. *Pharmacogn Mag.* 13, S737–S741 (2018).
- 18. Abbas, Z. et al. Radical scavenging potential of spectrophotometric, spectroscopic, microscopic, and EDX observed zinc oxide nanoparticles from leaves, buds, and flowers extract of *Bauhinia variegata* Linn: A thorough comparative insight. *Microsc Res. Tech.* 87, 2121–2133 (2024).
- 19. Pani, S. R., Mishra, S., Sahoo, S. & Panda, P. K. Nephroprotective effect of *Bauhinia variegata* (Linn.) Whole stem extract against cisplatin-induced nephropathy in rats. *Indian J. Pharmacol.* 43, 200–202 (2011).
- 20. Chen, Y. F. et al. Partitioned extracts of *Bauhinia championii* induce G0/G1 phase arrest and apoptosis in human colon cancer cells. *Am. J. Chin. Med.* 48, 719–736 (2020).
- 21. Xu, W. et al. Extracts of *Bauhinia Championii* (Benth.) Benth. Attenuate the inflammatory response in a rat model of collagen-induced arthritis. *Mol. Med. Rep.* 13, 4167–4174 (2016).
- 22. Xu, W. et al. Extracts of *Bauhinia Championii* (Benth.) Benth. Inhibit NF-B-signaling in a rat model of collagen-induced arthritis and primary synovial cells. *J. Ethnopharmacol.* **185**, 140–146 (2016).
- Chávez-Bustos, E. A. et al. Bauhinia forficata Link, antioxidant, genoprotective, and hypoglycemic activity in a murine model. Plants (Basel) 11, 3052 (2022).
- 24. Tonelli, C. A. et al. Clinical efficacy of capsules containing standardized extract of *Bauhinia forficata* Link (pata-de-vaca) as adjuvant treatment in type 2 diabetes patients: a randomized, double blind clinical trial. *J. Ethnopharmacol.* 282, 114616 (2022).
- 25. Ferreira-Filho, J. C. C. et al. Therapeutic potential of *Bauhinia forficata* link in dental biofilm treatment. *J. Med. Food.* 23, 998–1005 (2020).
- 26. Franco, R. R. et al. Antidiabetic potential of *Bauhinia forficata* Link leaves: A non-cytotoxic source of lipase and glycoside hydrolases inhibitors and molecules with antioxidant and antiglycation properties. *Biomed. Pharmacother.* 123, 109798 (2020).
- 27. Bubser, M., Byun, N., Wood, M. R. & Jones, C. K. Muscarinic receptor pharmacology and circuitry for the modulation of cognition. *Handb. Exp. Pharmacol.* 121–166 (2012).
- 28. Knorr, D. Y., Georges, N. S., Pauls, S. & Heinrich, R. Acetylcholinesterase promotes apoptosis in insect neurons. *Apoptosis* 25, 730–746 (2020).
- 29. Knorr, D. Y., Demirbas, D. & Heinrich, R. Multifaced promotion of apoptosis by acetylcholinesterase. Front. Cell. Death 2, 1169966 (2023).
- 30. Lozano, G. M. et al. Relationship between caspase activity and apoptotic markers in human sperm in response to hydrogen peroxide and progesterone. *J. Reprod. Dev.* **55**, 615–621 (2009).
- 31. Deng, S. et al. Albumin reduces oxidative stress and neuronal apoptosis via the ERK/Nrf2/HO-1 pathway after intracerebral hemorrhage in rats. Oxid. Med. Cell. Longev 8891373 (2021).
- 32. Radi, E., Formichi, P., Battisti, C. & Federico, A. Apoptosis and oxidative stress in neurodegenerative diseases. *J. Alzheimers Dis.* 42(Suppl 3), S125–S152 (2014).
- 33. Knopman, D. S. et al. Alzheimer disease. Nat. Rev. Dis. Primers. 7, 33 (2021).
- 34. Jahn, H. Memory loss in Alzheimer's disease. Dialogues Clin. Neurosci. 15, 445-454 (2013).
- 35. Ghafarimoghadam, M. et al. A review of behavioral methods for the evaluation of cognitive performance in animal models: current techniques and links to human cognition. *Physiol. Behav.* **244**, 113652 (2022).
- 36. Dalkiran, B., Açıkgöz, B. & Dayi, A. Behavioral tests used in the evaluation of learning and memory in experimental animals. *J. Basic. Clin. Health Sci.* 6, 938–945 (2022).
- 37. Bartus, R. T., Dean, R. L., Beer, B. & Lippa, A. S. The cholinergic hypothesis of geriatric memory dysfunction. *Science* 217, 408–414 (1982).
- 38. Li, Y. et al. Circular RNA expression profile of Alzheimer's disease and its clinical significance as biomarkers for the disease risk and progression. *Int. J. Biochem. Cell. Biol.* **123**, 105747 (2020).

- 39. Solari, N. & Hangya, B. Cholinergic modulation of spatial learning, memory and navigation. Eur. J. Neurosci. 48, 2199–2230 (2018)
- 40. Cassity, S. et al. Cholinergic modulation of rearing in rats performing a spatial memory task. Eur. J. Neurosci. 59, 2240-2255 (2024).
- 41. Singh, S. P. & Gupta, D. Discovery of potential inhibitor against human acetylcholinesterase: A molecular docking and molecular dynamics investigation. *Comput. Biol. Chem.* 68, 224–230 (2017).
- 42. Auld, D. S., Kornecook, T. J., Bastianetto, S. & Quirion, R. Alzheimer's disease and the basal forebrain cholinergic system: Relations to beta-amyloid peptides, cognition, and treatment strategies. *Prog Neurobiol.* **68**, 209–245 (2002).
- Roy, R., Niccolini, F., Pagano, G. & Politis, M. Cholinergic imaging in dementia spectrum disorders. Eur. J. Nucl. Med. Mol. Imaging 43, 1376–1386 (2016).
- 44. Wilson, D. M. et al. Hallmarks of neurodegenerative diseases. Cell 186, 693-714 (2023).
- 45. Goel, P. et al. Neuronal cell death mechanisms in Alzheimer's disease: An insight. Front. Mol. Neurosci. 15, 937133 (2022).
- 46. DeTure, M. A. & Dickson, D. W. The neuropathological diagnosis of Alzheimer's disease. Mol. Neurodegener. 14, 32 (2019).
- 47. Arendt, T., Brückner, M. K., Morawski, M., Jäger, C. & Gertz, H. J. Early neurone loss in Alzheimer's disease: Cortical or subcortical. Acta Neuropathol. Commun. 3, 10 (2015).
- 48. Chandrasekhar, Y., Kumar, P., Ramya, G., Anilakumar, K. R. & E.M., & Gallic acid protects 6-OHDA induced neurotoxicity by attenuating oxidative stress in human dopaminergic cell line. *Neurochem Res.* 43, 1150–1160 (2018).
- Javaid, N. et al. Neuroprotective effects of ellagic acid in Alzheimer's disease: Focus on underlying molecular mechanisms of therapeutic potential. Curr. Pharm. Des. 27, 3591–3601 (2021).
- 50. Chen, X., Guo, C. & Kong, J. Oxidative stress in neurodegenerative diseases. Neural Regen Res. 7, 376-385 (2012).
- 51. Butterfield, D. A., Swomley, A. M. & Sultana, R. Amyloid β-peptide (1–42)-induced oxidative stress in Alzheimer disease: Importance in disease pathogenesis and progression. *Antioxid. Redox Signal.* **19**, 823–835 (2013).
- 52. Anoush, M. et al. *Thymus daenensis* extract prevents scopolamineinduced memory impairment through declining oxidative stress in rats. *Acta Neurobiol. Exp. (Wars)* 82, 380–388 (2022).
- 53. Foyet, H. S., Abaïssou, H. H., Wado, E., Acha, E. A. & Alin, C. *Emilia coccinae* (SIMS) G extract improves memory impairment, cholinergic dysfunction, and oxidative stress damage in scopolamine-treated rats. *BMC Complement. Altern. Med.* 15, 333 (2015).
- Ferdous, R. et al. Anticholinesterase and antioxidant activity of *Drynaria Quercifolia* and its ameliorative effect in scopolamineinduced memory impairment in mice. *J. Ethnopharmacol.* 319, 117095 (2024).
- 55. Naudí, A. et al. Lipidomics of human brain aging and Alzheimer's disease pathology. Int. Rev. Neurobiol. 122, 133-189 (2015).
- 56. Wei, J., Wong, L. C. & Boland, S. Lipids as emerging biomarkers in neurodegenerative diseases. Int. J. Mol. Sci. 25, 131 (2023).
- Qizilbash, N. et al. Cholinesterase inhibition for Alzheimer disease: A meta-analysis of the tacrine trials. *Dement. Trialists' Collab. JAMA* 280, 1777–1782 (1998).
- 58. Tacrine (Discontinued)-Cognex. *Medscape Reference*. WebMD. Archived from the original on 30 June 2019. Retrieved 8 October (2013).
- 59. Kumari, E., Li, K., Yang, Z. & Zhang, T. Tacrine accelerates spatial long-term memory via improving impaired neural oscillations and modulating GAD isomers including neuro-receptors in the hippocampus of APP/PS1 AD mice. *Brain Res. Bull.* 161, 166–176 (2020).
- 60. Manning, F. C. Tacrine therapy for the dementia of Alzheimer's disease. Am. Fam. Physician 50, 819-826 (1994).
- 61. Kozurkova, M., Hamulakova, S., Gazova, Z., Paulikova, H. & Kristian, P. Neuroactive multifunctional tacrine congeners with cholinesterase, anti-amyloid aggregation and neuroprotective properties. *Pharmaceuticals* 4, 382–418 (2011).
- 62. Sohn, E., Kim, B. Y., Kim, Y. J. & Jeong, S. J. Non-clinical safety assessment of *Annona atemoya* leaf extract: Evaluation of genotoxicity. *Toxicol. Res.* 40, 473–485 (2024).
- 63. De Hoon, M. J., Imoto, S., Nolan, J. & Miyano, S. Open source clustering software. Bioinformatics 20, 1453-1454 (2004).
- 64. Kim, B. Y. et al. Neurodegenerative pathways and metabolic changes in the hippocampus and cortex of mice exposed to urban particulate matter: Insights from an integrated interactome analysis. Sci. Total Environ. 945, 173673 (2024).
- 65. Csardi, G. & Nepusz, T. The igraph software package for complex network research. Int. J. Complex. Syst. 1695, 1-9 (2006).
- 66. Oughtred, R. et al. The BioGRID interaction database: 2019 update. Nucleic Acids Res. 47, D529-D541 (2019).

#### Author contributions

E.S. wrote the manuscript and performed the animal experiments and analysis. B.Y.K. wrote the manuscript and performed the RNA sequencing analysis. Y.J.K. prepared the sample extract and collaborated in the animal experiments. J.H.K. prepared the sample extract. S.J.J. conceptualized and supervised the study, and wrote the manuscript. All authors reviewed the manuscript.

# **Funding**

This work was supported by the Korea Institute of Oriental Medicine (KSN1515293 and KSN2411012) and the National Research Foundation of Korea (NRF) (NRF-2020R1A2C2012917) funded by the Ministry of Science and ICT (MSIT), Republic of Korea, and conducted at the Korea Institute of Oriental Medicine (NSN2015400).

# **Declarations**

# Competing interests

The authors declare no competing interests.

#### Additional information

**Supplementary Information** The online version contains supplementary material available at https://doi.org/1 0.1038/s41598-025-88152-8.

Correspondence and requests for materials should be addressed to S.-J.J.

Reprints and permissions information is available at www.nature.com/reprints.

**Publisher's note** Springer Nature remains neutral with regard to jurisdictional claims in published maps and institutional affiliations.

Open Access This article is licensed under a Creative Commons Attribution-NonCommercial-NoDerivatives 4.0 International License, which permits any non-commercial use, sharing, distribution and reproduction in any medium or format, as long as you give appropriate credit to the original author(s) and the source, provide a link to the Creative Commons licence, and indicate if you modified the licensed material. You do not have permission under this licence to share adapted material derived from this article or parts of it. The images or other third party material in this article are included in the article's Creative Commons licence, unless indicated otherwise in a credit line to the material. If material is not included in the article's Creative Commons licence and your intended use is not permitted by statutory regulation or exceeds the permitted use, you will need to obtain permission directly from the copyright holder. To view a copy of this licence, visit <a href="http://creativecommons.org/licenses/by-nc-nd/4.0/">http://creativecommons.org/licenses/by-nc-nd/4.0/</a>.

© The Author(s) 2025